Available online at www.sciencedirect.com
ScienceDirect
Journal of Hazardous Materials 153 (2008) 418–425
Journal of Hazardous Materials
www.elsevier.com/locate/jhazmat

Comparison of the properties of glass, glass–ceramic and ceramic materials produced from coal fly ash

M. Erol *, S. Küçükbayrak, A. Ersoy-Meriçboyu

Department of Chemical Engineering, Chemical & Metallurgical Engineering Faculty, Istanbul Technical University, Maslak 34469, Istanbul, Turkey

Received 31 May 2007; received in revised form 8 August 2007; accepted 27 August 2007
Available online 31 August 2007

Abstract

Glass, glass–ceramic and ceramic materials were produced from thermal power plant fly ash without any additives. X-ray diffraction (XRD) analysis revealed the amorphous phase of the glass sample. Augite phase was detected in the glass–ceramic sample, while the enstatite and mullite phases occurred in the ceramic samples. Scanning electron microscopy (SEM) investigations showed that tiny crystallites homogeneously dispersed in the microstructure of the glass–ceramic sample and elongated crystals formed in the ceramic samples. Density values of the obtained samples are comparable to those of the commercially produced glass, glass–ceramic and ceramic samples. Toxicity characteristic leaching procedure (TCLP) results indicated that the produced samples could be taken as non-hazardous materials. Produced samples showed high resistance to alkali solutions in contrast to acidic solutions. Microstructural, physical, chemical and mechanical properties of the produced glass–ceramic samples are better than those of the produced glass and ceramic samples.

Keywords: Coal fly ash; Glass; Glass–ceramic; Ceramic

1. Introduction

In recent years, there has been considerable interest in environmental problems in the worldwide; therefore, many researchers have paid much attention to find permanent solutions for the recycling of industrial hazardous wastes. One of the major wastes is coal fly ash, which is produced in significant amounts in the world. The increasing production of coal fly ash waste from thermal power plants has compounded environmental and economical problems worldwide. Storage of this waste has recently become more restricted because of increasing regulatory laws and the increasing costs of landfilling [1]. Currently, large quantities of fly ash are used for landfilling which cause negative environmental impacts such as leaching of potentially toxic substances into soil and groundwater, the change in the elemental composition of the vegetation growing in the vicinity of the ash and the accumulation of toxic elements throughout the food chain [2]. Industrial activities pertinent to the utilization of fly ash into useful articles have received worldwide popularity in the last four decades in many areas mainly in the construction sector [3].

The physical and chemical properties of fly ash depend on the type of coal used and the combustion conditions. Fly ash, which exists in different particle sizes (between 1 and 100 μm) and shapes, is made up of tiny glass beads and depending on the chemical composition; its color varies from pale brown to gray [2]. Fly ash contains valuable oxide resources such as SiO_2, Al_2O_3, CaO, Fe_2O_3, and other oxides. These oxides have been mainly considered as a low cost material resource for the glass, glass–ceramic and ceramic industry. Moreover, fly ash is presented as a fine dust so it can be directly used in the production of these materials, with almost no pre-treatment.

Both vitrification and sintering of hazardous wastes into glass, glass–ceramic and ceramic materials provide an alternative way to waste treatment or landfilling. The produced materials seem promising, not only because of their outstanding properties, but also since the hazardous wastes can be successfully converted into glass, glass–ceramic and ceramic products as non-hazardous materials. Recycling of hazardous wastes in glass, glass–ceramic and ceramic production results in three

* Corresponding author. Tel.: +90 212 285 3351; fax: +90 212 285 2925.
E-mail address: erolm@itu.edu.tr (M. Erol).

0304-3894/$ – see front matter © 2007 Elsevier B.V. All rights reserved.
doi:10.1016/j.jhazmat.2007.08.071

main advantages; first the use of a zero cost raw material, second, the conservation of natural resources, and thirdly, the elimination of the waste with the protection of the environment [4].

There has been considerable research on the production of glass [5], glass–ceramic [1,6–11] and ceramic [12–15] materials from coal fly ash without or with the addition of natural raw materials and wastes such as glass cullet, dolomite slag and tincal ore waste in the last few decades. However, there has not been paid much attention to obtain glass, glass–ceramic and ceramic materials by using only one material source, coal fly ash.

The present study aims to investigate the possibility of producing glass, glass–ceramic and ceramic materials from one coal fly ash sample without any additives or nucleating agents in order to establish the best conditions to obtain products with desirable properties suitable for construction sector.

2. Experimental procedure

2.1. Starting material

The fly ash sample used in this study was obtained from Tunçbilek thermal power plant in Turkey. The chemical analyses of fly ash were carried out according to ASTM standards [16,17]. Table 1 shows the chemical composition and loss of ignition value (LOI) of fly ash sample. Heavy metals detected in coal fly ash were also given in Table 1.

X-ray diffraction was utilized to determine the mineralogical properties of the fly ash. During the combustion process, temperature may exceed 1873 K. This temperature is sufficiently high to melt most of the inorganic materials present in the coal fly ash. The majority of the minerals formed were quartz (SiO_2), mullite ($Al_6Si_2O_{13}$), enstatite ($(Mg, Fe)SiO_3$), hematite (Fe_2O_3) and anorthite ($CaAl_2Si_2O_8$) (Fig. 1a).

The average particle size was determined using a Shimadzu centrifugal particle size analyzer (SA-CP3 Model) and the density of fly ash sample was determined by means of mercury porosimeter. The average particle size and the density of fly ash sample were 91 μm and 1.89 g/cm^3, respectively. Coal fly ash sample was in a fine powder form.

2.2. Glass preparation

Glass sample was prepared from the fly ash without any additives. In each batch 20 g of fly ash was melted in platinum crucible for 2 h in an electrically heated furnace (Protherm PLF 1600 Model) at 1773 K. To ensure homogeneity, the melt was poured into water. The cast glass was crushed, pulverized and remelted at the same temperature for 3 h to remove the air bubbles from the melt. Following this procedure, the refined melt was cast in a preheated graphite mould (673 K) to form

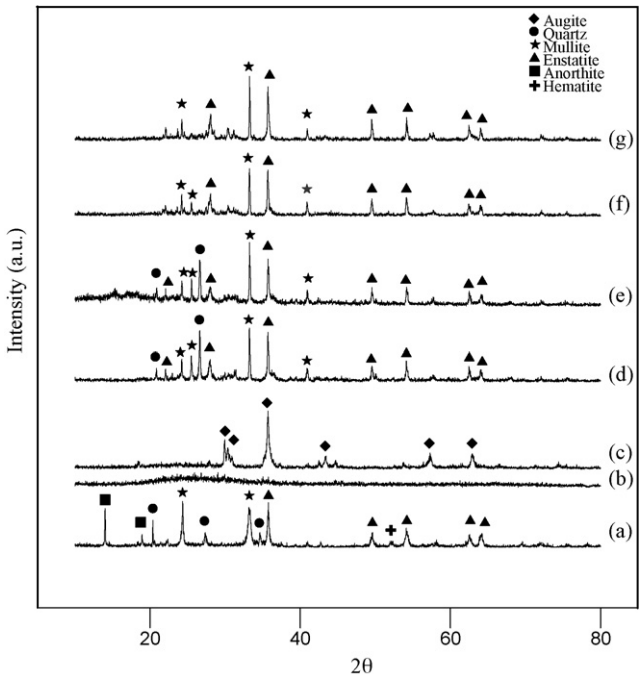

Fig. 1. XRD patterns of Tunçbilek fly ash and the produced samples: (a) fly ash, (b) TG, (c) TGC, (d) TFA1398, (e) TFA1423, (f) TFA1448 and (g) TFA1473.

cylinders of approximately 0.8–1 cm in diameter and 1–4 cm in length. The cylinders were cooled to room temperature. To remove thermal residual stress, the cast glass was annealed in a furnace at 873 K for 2 h followed by slow cooling to room temperature. The annealing temperature was chosen as 873 K since 70–100 K below the glass transition temperature is appropriate for the annealing temperature as reported in the literature [6,18]. The annealing time of 2 h was determined as an optimum time in a previous study [19].

2.3. Glass–ceramic production

Annealed glass sample was subjected to a one-stage heat treatment process to obtain glass–ceramic material. The heat treatment temperature that was above the crystallization peak temperature was selected on the basis of DTA result obtained in a previous study [20]. Annealed glass sample was heated at a rate of 10 K/min to 1423 K and held at this temperature for 2 h. The produced sample was then cooled in the furnace.

2.4. Ceramic production

Tunçbilek thermal power plant fly ash was sintered to form ceramic materials using conventional powder processing technique based on powder compaction and firing, without the

Table 1
Chemical analysis of fly ash sample

	SiO_2 (%)	Al_2O_3 (%)	CaO (%)	MgO (%)	Fe_2O_3 (%)	Na_2O (%)	K_2O (%)	SO_3 (%)	LOI (%)	Cr^{3+} (ppm)	Pb^{2+} (ppm)	Mn^{2+} (ppm)	Zn^{2+} (ppm)
Tunçbilek fly ash	57.01	21.28	2.98	3.19	10.61	0.47	1.15	1.73	0.78	20.30	11.70	10.50	28.70

addition of organic binder or inorganic additives. In sample preparation, a small amount of water was used to humidify the fly ash before compaction. 1.5 g of fly ash was mixed in a mortar with water at the water/solid ratio of 0.1 for each pellet. The circular pellets of 10 mm diameter were uniaxially pressed at 40 MPa to achieve a reasonable strength. The powder compacts were sintered in air. A number of preliminary experimental trials were conducted on fly ash sample at different heating temperatures and residence times in order to investigate the possibility of thermal treatment of fly ash alone. The firing temperatures and the residence time, which were selected on the basis of preliminary runs, are 1398–1473 K and 2 h, respectively. Firing experiments were carried out in the Protherm PLF 1600 furnace equipped with a small chamber and a programmable controller (the internal PID constants were adjusted to obtain a maximum deviation of 7 K). Before every sintering operation the samples were pre-heated to 573 K for 60 min to derive off adsorbed gasses and moisture. After that, the temperature was raised to the firing temperature. The heating rate was 10 K/min and the sintering time was 120 min for all samples. All samples were cooled down in the furnace.

2.5. Characterization of the produced glass, glass–ceramic and sintered materials

X-ray diffraction was utilized to determine the crystalline phases occurred in the produced samples. The initial glass composition was analyzed to check for any crystalline phases that may have formed during annealing process. In all cases, samples, which were analyzed by X-ray diffraction, were ground to fine powder form. A Siemens diffractometer Model D 5000 operated at 40 kV and 30 mA utilizing Cu Kα radiation was used for the measurements. The detector was scanned over a range of 2θ angles from 10 to 80°, at a step size of 0.02° and a dwell time of 2 s per step.

In this study, Amray Model 1830 operated at 20 kV was used to observe the microstructure of the produced samples. Samples were mounted (using Buehler Model Simpliment II) in epoxy resin and their surfaces were ground flat by 400, 800, 1000 and 1200 grit abrasive papers. Then the samples were polished with diamond paste to achieve a mirror-smooth surface. The polished samples were etched with HF solution (5 volume%) for 1.5 min, immediately rinsed with excess distilled water and then cleaned in ethanol for 2 min. The samples were coated with carbon prior to examination.

Vickers microhardness values of the produced glass and glass–ceramic samples were determined. The microhardness tester used in this study was a Leco Model M-400-G. Samples were ground and polished with diamond paste. A load of 0.5 kg was selected and the time of indentation was fixed as 15 s.

Rockwell hardness measurements were done on the ceramic materials produced from fly ash to determine the effects of different heat treatment processes on the mechanical properties of the samples. The Rockwell hardness tester used in this study was a Wilson Model 4J. The hardness of the produced ceramic materials was determined by the Rockwell hardness test, according to the specifications of ASTM E-18 [21]. A superficial Rockwell Hardness tester (Wilson) was employed with 1.588 mm ball indenter (*B* scale) to the ceramic materials loading at a minor load of 0.5 kg and major load of 1 kg.

The water absorptions (%) of the produced materials were determined using the procedure outlined in the ASTM standards [22]. Water absorption data is the indication of open, water accessible porosity. Density and the total porosity of the produced glass, glass–ceramic and ceramic materials were measured by using a Quantachrome Autoscan-33 mercury porosimeter. Mercury intrusion porosimetry measurements of the samples were carried out pressurizing up to 227 MPa with an Hg contact angle of 140°. Mercury intrusion to the samples takes place with the increase of pressure. Data on density and total porosity were acquired through a microcomputer data acquisition system interfaced with the porosimeter.

Toxicity evaluation was made by application of standard leaching procedures. In order to assess the stabilization of the coal fly ash into glass, glass–ceramic and ceramic materials, the produced samples were subjected to TCLP test. The experimental procedure according to TCLP is summarized as follows [23]: one leaching solution (extraction fluid) was used in the experiments. Extraction fluid consists of 5.7 ml of acetic acid diluted in 500 ml of distilled water, in which 64.3 ml of NaOH (1 M) were added and the resulting solution was diluted with distilled water to the volume of 1 l giving a final pH value of 4.93 ± 0.05. The produced samples were manually crushed (<9.5 mm) and placed in a conical flask. Extraction fluid was added in order to keep a liquid to solid ratio of 20 ($L/S = 20$). The flask is tightly closed and stored at 298 K for 18 h. The resultant solutions were filtered through a 0.6 and 0.8 μm filters and the concentrations of heavy metals in the leachate were determined by using inductively coupled plasma (ICP). A Perkin-Elmer Model Optima 3000 XL ICP operated at 13.56 MHz (using Ar and N_2 gases) was used for the measurements.

The chemical resistances of the glass, glass–ceramic and ceramic materials were estimated in 10% HNO_3 and 10% NaOH solutions. In these experiments, 2 g of grained samples with particle size between 0.3 and 0.5 mm were treated at 373 K for 2 h in 70 ml solutions. After washing and drying, the grained samples were weighed and the percentages of mass losses were calculated.

3. Results and discussion

Coal fly ash was used to produce glass, glass–ceramic and ceramic materials. Visual inspections of the color and texture of the produced samples showed that obtained glass sample was shiny black color with a smooth surface. The produced glass–ceramic sample had also smooth surface and the color of the sample was dark black. The dark red color of the pressed fly ash sample became brown after the sintering process. The rough surface of the pressed fly ash sample was getting smoother and further increase in the sintering temperature caused to shiny glassy texture on the surface of the ceramic samples. The applied heat treatment schedules to the

Table 2
Codes of the produced samples

Material	Heat treatment time (h)	Heat treatment temperature (K)	Codes of the samples
Glass	2	873	TG
Glass–ceramic	2	1423	TGC
Ceramic	2	1398	TFA1398
		1423	TFA1423
		1448	TFA1448
		1473	TFA1473

samples and the codes of the produced materials were given in Table 2.

3.1. XRD studies of the produced samples

XRD pattern of the TG sample shown in Fig. 1 indicated the amorphous state of the sample. As seen from Fig. 1b, the spectra show presence of a non-crystalline material and absence of any distinct crystalline species, as it was expected.

In order to identify the crystalline phase(s), X-ray scans were also carried out on glass–ceramic sample. The XRD analysis of TGC sample is shown in Fig. 1c. There is no doubt that crystalline phase coexist since the XRD patterns show that the amorphous phase has practically disappeared and aluminum augite ($Ca(Mg, Fe^{3+}, Al)(Si, Al)_2O_6$) phase occurred in the sample.

The crystalline phases occurred in the sintered TFA samples changed with the increase in the firing temperature. As seen from Fig. 1d–g, the intensity and the location of the peaks changed. Both anorthite and hematite phases disappeared when the fly ash sample heat-treated at 1398 K. Quartz (SiO_2) mullite ($Al_6Si_2O_{13}$) and enstatite ($(Mg, Fe)SiO_3$) phases can be seen from Fig. 1d. When the sintering temperature increased to 1448 K the quartz peak at 27° 2θ disappeared in the XRD pattern of TFA1448 sample. At 1473 K, enstatite and mullite phases are the two main phases in the microcrystalline structure of the TFA1473 sample. High Al_2O_3–SiO_2 content of Tunçbilek fly ash caused the mullite phase while the enstatite phase was an indicative of high Fe_2O_3 content of it.

3.2. SEM studies of the produced samples

The microstructural studies were performed on the obtained glass samples using SEM. The homogeneity of waste glass was obviously related to the performance of the production process. SEM investigations confirmed the homogeneous nature of the produced glass sample. Fig. 2 indicates the SEM micrograph of the TG sample. TG sample had smooth surface and were bubble free.

SEM micrograph of the TGC sample (Fig. 3) shows the presence of strongly interlocked tiny crystals of about 0.15–0.30 μm size embedded in a glassy matrix and the absence of pores. The controlled nucleation and crystallization of glasses is of prime importance in the formation of glass–ceramics, because the properties are influenced by the manner in which crystallization occurs. According to the conventional process, the production of a glass–ceramic material involves two steps: a low temperature heat treatment of glass, to induce nucleation, followed by heating to a second, higher temperature, to allow crystal growth of the nuclei. In this case the controlled heat treatment process was not applied to the glass sample. However, TGC sample had a good microcrystalline structure with homogeneously dispersed tiny crystallites. Microstructure of TGC sample is good enough comparing to the glass–ceramics that were produced from TG sample by applying controlled heat treatment process in the previous study [20].

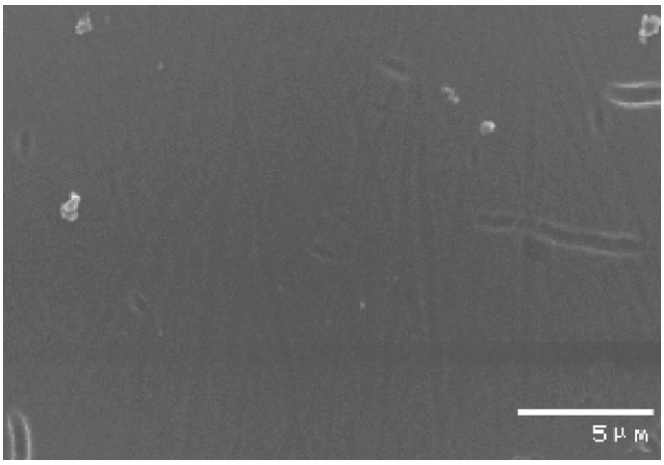

Fig. 2. SEM micrograph of the TG sample.

To investigate the microstructural evolution, SEM was conducted on the sintered TFA samples. Figs. 4–7 are the representative SEM micrographs of the TFA1398, TFA1423, TFA1448 and TFA1473 samples, respectively. It was clearly seen from Fig. 4 that small amount of crystallites occurred in the glassy matrix. The size of the elongated crystallites was between 4 and 7 μm in length. The elongated crystallites gathered to form a bigger crystalline size. These gathered crystallites were surrounded by the glassy phase. Fig. 5 shows the gathered crystallites and the size of the elongated crystallites was in the range of 4–8 μm in length. The microstructures of the TFA1398 and TFA1423 are very similar to each other. Microstructure of

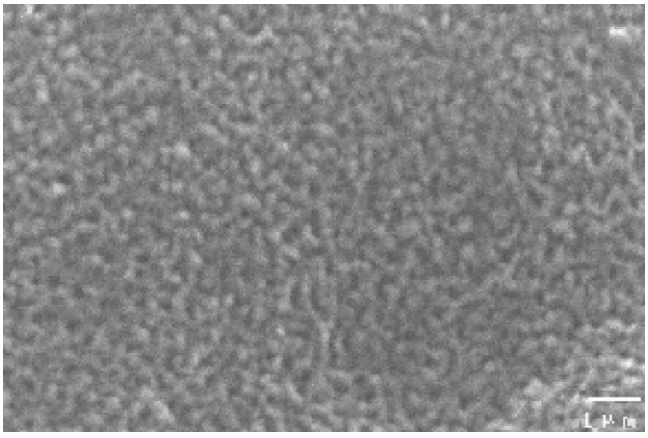

Fig. 3. SEM micrograph of the TGC sample.

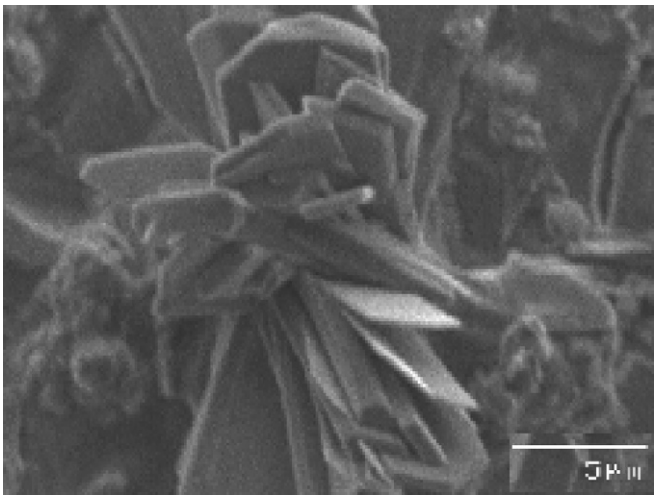

Fig. 4. SEM micrograph of TFA1398 sample.

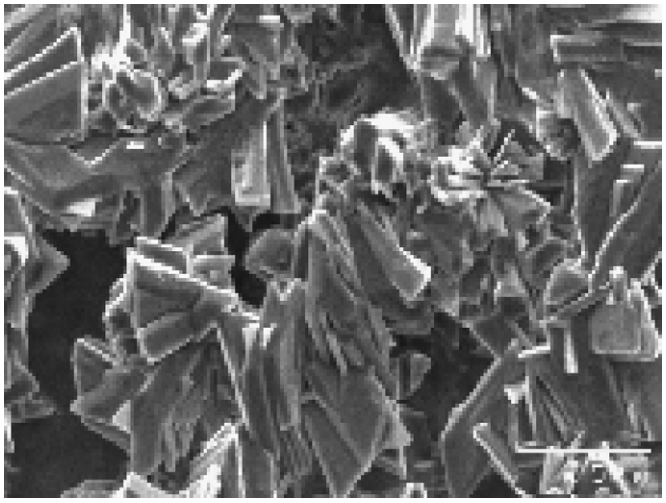

Fig. 6. SEM micrograph of TFA1448 sample.

the sintered TFA samples changed when the sintering temperature was raised. As seen from Fig. 6, more elongated crystallites dispersed in the microstructure of the TFA1448 sample. The amount of the crystallites increased while the crystalline size decreased with the increase in sintering temperature. The crystalline sizes are varied between 2 and 5 μm. Fig. 7 shows the SEM micrograph of the TFA1473 sample. The crystalline size and the shape were similar with the crystallites formed in the TFA1448 sample. However, the microcrystalline structure was denser than the microstructure of TFA1448 sample. The amount of the crystallites increased in the TFA1473 sample. The elongated crystallites interlocked together to form a more dense crystalline structure. Small amount of glassy phase still remained in the microstructure of the TFA1473 sample. SEM observations revealed that more dense crystalline structure occurred with the increase in sintering temperature.

3.3. Physical and mechanical properties of the produced samples

Porosity, density, water adsorption and hardness values of the produced samples were given in Table 3. Density and hardness values of the glass sample were found as 2.91 g/cm^3 and 511 kg/mm^2, respectively. Density value of TG sample is better than those of the glasses produced from wastes such as coal fly ash and incinerator fly ash [7,8,24]. High density value of TG sample is also an indicator of the low water absorption and porosity values of the produced glasses. Microhardness value of TG sample is high in comparison with window glass (418.1 kg/mm^2), silica glass (476.7 kg/mm^2) [25], glasses produced from coal fly ash in another study (410 kg/mm^2) [8] and

Table 3
Properties of the produced samples

Sample code	Vickers microhardness (kg/mm^2)	Rockwell hardness	Density (g/cm^3)	Porosity (%)	Water absorption (mass% loss)
TG	511	–	2.91	0.31	0.10
TGC	792	–	3.19	0.01	0.03
TFA1398	–	40	1.93	15.30	13.20
TFA1423	–	43	2.03	12.10	9.70
TFA1448	–	53	2.17	8.60	6.78
TFA1473	–	58	2.37	6.30	5.12

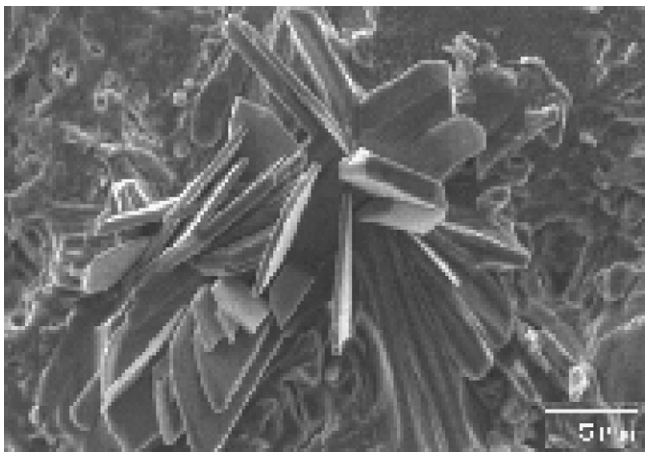

Fig. 5. SEM micrograph of TFA1423 sample.

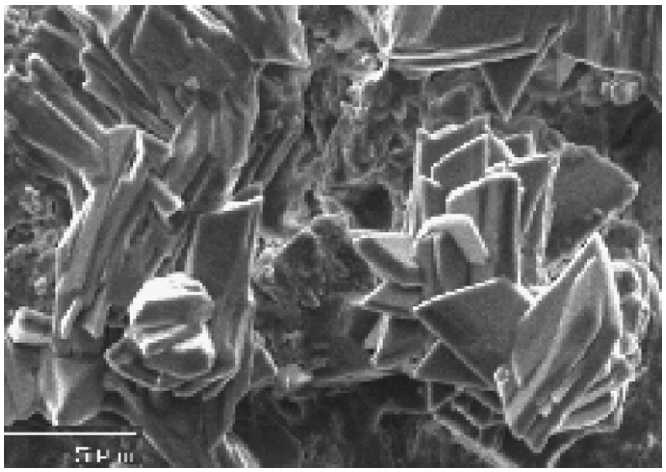

Fig. 7. SEM micrograph of TFA1473 sample.

glasses produced from municipal solid waste (MSW) incinerator fly ash (482.3 kg/mm^2) [26].

Density of the glass–ceramic sample is 3.19 g/cm^3 and this value is higher than that of TG sample. Density increased with increasing crystalline volume in the glassy matrix. SEM and XRD results showed that TG sample had amorphous glassy structure while TGC sample had fully crystallized structure. Similar to density results, as TGC sample had crystalline structure, the hardness increased, the porosity and water absorption decreased. Physical and mechanical properties of the TGC sample are better than the properties of glass–ceramic materials produced from incinerator fly ash [27,28]. According to Cheng et al., the highest hardness value of the gehlenite glass–ceramic was 479 kg/mm^2 [28]. Hardness value of TGC sample is higher than that value.

The properties of the produced ceramic materials were also given in Table 3. Density values increased from 1.93 to 2.37 g/cm^3 during the thermal treatment of the samples. Density is a parameter that can be used as an indicator of the degree of sintering. Increasing of density values is a result of more dense crystalline structure with a less glassy phase and porosity. Therefore, with the increase in density values the water absorption and porosity values are also decreased. Water absorption data demonstrates the reduction in open, water accessible porosity with increased firing temperature. The water absorption values increased with the decrease in the sintering temperature. In compliance with the water absorption values, total porosity values decreased with increasing sintering temperature. The high water absorption and total porosity values of TFA samples decreased from 13.20 to 5.12% and 15.30 to 6.30%, respectively. As it was expected; open, water accessible porosity values are lower than those of the total porosity values of the samples. The lowest porosity and water absorption values of the TFA1473 sample are indicatives of dense well-sintered microstructure with a minimum volume of porosity. The porosity values of TFA samples are higher than those of the TG and TGC samples. This is believed to result from simultaneous evaluation of gases at relatively low sintering temperatures comparing to high melting temperature of glass. The density values of TFA samples are higher than the density values of sintered fly ash samples produced by Artır et al. [12], Polettini et al. [29] and Lingling et al. [13]. The water adsorption and the porosity values were also better than the values reported by Lingling et al. [13] and Artır et al. [12].

The Rockwell hardness values increased with the increase in sintering temperatures as it was observed in the density values. From SEM observations, we can clearly see that the average crystal sizes of both TFA1448 and TFA1473 samples were smaller than the other samples and the hardness values were better. It was reported in the literature that the fine-grained ceramic materials possess better hardness property together with finer crystal size [9]. It is obvious that the TFA1473 sample had more dense microcrystalline structure with better physical and mechanical properties than those of the other TFA samples.

Density value is a function of both the crystalline sizes and the crystalline volume in the glassy matrix. SEM observations and XRD results indicated that TGC sample had higher crystalline degree with small crystalline sizes in all produced samples. Both porosity and water absorption are correlated well each other and decreased with the increase of the crystalline sites. However, physical properties of the amorphous TG sample are better than the crystalline TFA samples. This result can be explained with the sintering conditions. Sintering mechanism is controlled by impurities, surface area, packing efficiency and crystallization behavior. The driving force for sintering of fly ash particles is reduction of surface area. Increasing the surface area tends to promote sintering. The surface area is increased by decrease in the particle size. Another important parameter that affects sintering is how well the particles are initially packed together. Increasing the packing density promotes sintering. In the cold pressing technique, the sintering pressure is very important to get better initially packed fly ash particles. Sintering can also be enhanced by additions of binders. Binders can promote sintering, but usually also increase the cost and complexity of the materials system. According to the above discussions, high porosity and low density values obtained for the TFA samples since the selected sintering pressure and the particle size of the sample may not be suitable for the production of ceramic materials from Tunçbilek fly ash. And binderless working can also be another factor that resulted to the low density values for TFA samples. From Table 3, it is obvious that TGC sample has the best properties with the best microcrystalline structure.

3.4. TCLP results of the produced samples

The TCLP test was conducted to study the heavy metals migration. In this study, the TCLP analyses were limited to the main hazardous heavy metals of Zn, Pb, Mn and Cr. TCLP results of the produced samples from fly ash were given in Table 4. The results were compared with the US EPA limits. It was found that the extracted amounts of heavy metals are lower than the limits required by the US EPA. It should be noted that the volatile metals such as Zn and Pb may evaporate to the atmosphere before or during melting stage. Therefore, to treat fly ashes by using thermal melting technology, a secondary air pollution control system should be designed to catch volatile metals [27]. Another reason for the lower leachability is due to the heavy metal ions replaced with other ions and successfully solidified into the structures of the produced samples. Among the studied heavy metals, only Zn showed a leachable fraction, since Zn is unstable in acidic solutions and also Zn concentration is the highest in all heavy metal concentrations.

In order to interpret the TCLP results, the strong effect of microcrystalline structure formed in the samples should be taken into consideration. It was reported that crystalline structure

Table 4
TCLP results of the produced samples

Sample code	Cr^{3+} (ppm)	Mn^{2+} (ppm)	Zn^{2+} (ppm)	Pb^{2+} (ppm)
TG	BDL	BDL	0.005	BDL
TGC	BDL	BDL	BDL	BDL
TFA1473	BDL	BDL	0.003	BDL
US EPA limit	5	5	500	0.5

BDL: Below detection limit.

affects leaching resistance [30]. After formation of crystalline phases in the TGC and TFA samples, the products become more resistant to leaching comparing to the produced glass samples. It was obvious that the leaching resistance of TG sample was lower than the TGC and TFA samples. The heavy metal ions were strongly bonded inside the structure of the crystalline phases (augite, mullite and enstatite). The dissolution of the silica matrix can release heavy metals from the glass structure [5]. The bonds in the glass structure are weaker than the crystalline phases since the glasses are amorphous materials. Leaching resistance is also affected from microstructure of the samples. The better microcrystalline structure results the better leaching resistance. Therefore, TGC sample had the highest leaching resistance.

The glass sample produced in this work showed high leaching resistance than the glasses obtained from coal fly ash by Sheng et al. [5] and incinerator fly ash by Park and Heo [26]. TCLP results of the TGC and TFA samples are better than the results of the glass–ceramic materials produced from incinerator fly ash [31]. Cr-ion concentration in the resultant leachate solutions measured by Cheng [31] is higher than the concentration of the leachate solutions in this study.

3.5. Chemical resistance of the produced samples

Results for chemical resistance of the produced samples were given in Table 5. The chemical durability of produced samples shows acceptable behavior. However, they have relatively high mass losses for HNO_3 durability compare to NaOH durability. It is apparent that the produced samples show high resistance to alkali solutions. However, both HNO_3 and NaOH durabilities of TGC and TFA1473 samples are better than the glass–ceramic produced from coal fly ash according to the study which was reported by Leroy et al. [10]. It can be seen from Table 5 that the durabilities of the samples correlate well with the crystallization degree of the produced samples. Chemical resistance of TGC sample is the highest among all samples due to its better microcrystalline structure. Chemical resistance increased with decreasing amount of glassy matrix surrounding the crystalline grains. Since weight losses are usually attributed to the dissolution of the glassy matrix, this would lead to lower weight losses for TGC and TFA1473 samples than the other samples as it was expected. The improved property is attributed to the crystalline structure formed in the TGC and TFA samples.

Table 5
Chemical resistances of the produced samples

Sample code	Mass loss of samples (%) in solution	
	HNO_3	NaOH
TG	1.11	0.05
TGC	0.05	0.02
TFA1398	1.08	0.06
TFA1423	0.84	0.05
TFA1448	0.62	0.05
TFA1473	0.42	0.03

4. Conclusions

On the basis of the results reported in the present investigation, the following conclusions can be drawn:

1. Both SEM and XRD investigations indicated the amorphous glassy state of TG sample.
2. XRD analysis revealed that augite and enstatite + mullite phases occurred in the microstructure of the TGC and TFA samples, respectively.
3. SEM investigations showed that tiny crystallites were uniformly dispersed in the microstructure of TGC sample, while elongated mullite crystallites observed in the microstructure of TFA samples. On the basis of SEM and XRD analysis, it was observed that microstructures of the produced glass, glass–ceramic and ceramic materials produced from Tunçbilek fly ash were completely different from each other since the production methods of those materials were different.
4. Physical properties of TG and TGC samples are better than those of the produced ceramic samples since the coal fly ash particles were not initially packed together and therefore, particle coalescence could not be completely achieved during the sintering process.
5. TCLP results showed that the heavy metals of fly ashes were successfully immobilized into glass, glass–ceramic and ceramic samples.

Overall results showed that it is possible to produce glass, glass–ceramic and ceramic materials from Tunçbilek fly ash without any additives. It was also concluded that produced glass and glass–ceramic materials have several desirable properties that would make them attractive to industrial use in construction, tiling and cladding applications.

References

[1] L. Barbieri, I. Lancelotti, T. Manfredini, G.C. Pellaconi, J.M. Rincon, M. Romero, Nucleation and crystallization of new glasses from fly ash originating from thermal power plants, J. Am. Ceram. Soc. 84 (2001) 1851–1858.
[2] C.L. Carlsson, D.C. Adriano, Environmental impacts of coal combustion residues, J. Environ. Qual. 22 (1993) 227–247.
[3] O.E. Manz, Worldwide production of coal ash and utilization in concrete and other products, Fuel 76 (1997) 691–696.
[4] C. Ferreira, A. Ribeiro, L. Ottosen, Possible applications for municipal solid waste fly ash, J. Hazad. Mater. B96 (2003) 201–216.
[5] J. Sheng, B.X. Huang, J. Zhang, H. Zhang, J. Sheng, S. Yu, M. Zhang, Production of glass from coal fly ash, Fuel 82 (2003) 181–185.
[6] L. Barbieri, T. Manfredini, I. Queralt, J.M. Rincon, M. Romero, Vitrification of fly ash from thermal power stations, Glass Technol. 38 (1997) 165–170.
[7] J.M. Kim, H.S. Kim, Processing and properties of a glass-ceramic from coal fly ash from a thermal power plant through an economic process, J. Eur. Ceram. Soc. 24 (2004) 2825–2833.
[8] H. Shao, K. Liang, F. Zhaou, G. Wang, F. Peng, Characterization of cordierite-based glass–ceramics produced from fly ash, J. Non-Cryst. Sol. 337 (2004) 157–160.
[9] M.C. Ferro, C. Leroy, R.C.C. Monteito, M.H.V. Fernandes, Fine-grained glass-ceramics obtained by crystallization of vitrified coal ashes, Key Eng. Mater. 230–232 (2002) 408–411.

[10] C. Leroy, M.C. Ferro, R.C.C. Monteiro, M.H.V. Fernandes, Production of glass–ceramics from coal ashes, J. Eur. Ceram. Soc. 21 (2001) 195–202.
[11] F. Peng, K. Liang, A. Hu, Nano-crystal glass–ceramics obtained from high alumina coal fly ash, Fuel 84 (2005) 341–346.
[12] R. Artır, Ş. Yılmaz, C. Bindal, Some properties and sintering behavior of B_2O_3 added fly ash, Key Eng. Mater. 264–268 (2004) 2477–2480.
[13] X. Lingling, G. Wei, W. Tao, Y. Nanru, Study on fired bricks with replacing clay by fly ash in high volume ratio, Const. Build. Mater. 19 (2005) 243–247.
[14] A. Olgun, Y. Erdoğan, Y. Ayhan, B. Zeybek, Development of ceramic tiles from coal fly ash and tincal ore waste, Ceram. Inter. 31 (2005) 153–158.
[15] M. Ilic, C. Cheeseman, C. Sollars, J. Knight, Mineralogy and microstructure of sintered lignite coal fly ash, Fuel 82 (2003) 331–336.
[16] Annual Book of ASTM Standarts, 1984a, D3682-78 (1983) Standard test methods for major and minor elements in coal and coke ash by atomic absorption.
[17] Annual Book of ASTM Standarts, 1984b, D3683-78 (1983) Standard test methods for trace elements in coal and coke ash by atomic absorption.
[18] Ş. Yılmaz, O.T. Özkan, V. Günay, Crystallization kinetics of basalt glass, Ceram. Inter. 22 (1996) 477–481.
[19] M. Erol, S. Küçükbayrak, A. Ersoy-Meriçboyu, M.L. Öveçoğlu, Crystallization behavior of glasses produced from fly ash, J. Eur. Ceram. Soc. 21 (2001) 2835–2841.
[20] M. Erol, S. Küçükbayrak, A. Ersoy-Meriçboyu, Production of glass–ceramics obtained from industrial wastes by means of controlled nucleation and crystallization, Chem. Eng. J. 132 (2007) 335–343.
[21] Annual Book of ASTM Standarts, 2005, E-18, Standard Test Methods for Rockwell Hardness and Rockwell Superficial Hardness for Metallic Materials.
[22] Annual Book of ASTM Standards, 2000, C-20, Standard Test Methods for Apparent Porosity, Water Absorption, Apparent Specific Gravity and Bulk Density of Burned Refractory Brick and Shapes by Boiling Water.
[23] US EPA, 1992, US Environmental Protection Agency Method 1311 (Reviewed), Washington DC.
[24] A.R. Boccacini, M. Petitmermet, E. Wintermantel, Glass–ceramics from municipal incinerator fly ash, Am. Ceram. Soc. Bull. 97 (1997) 75–78.
[25] N.P. Bansal, R.H. Doremus, Handbook of Glass Properties, Academic Press, New York, 1985, pp. 223–377.
[26] Y.J. Park, J. Heo, Vitrification of fly ash from municipal solid waste incinerator, J. Hazard. Mater. B91 (2002) 83–93.
[27] T.W. Cheng, Effect of additional materials on the properties of glass–ceramic produced from incinerator fly ashes, Chemosphere 56 (2004) 127–131.
[28] T.W. Cheng, T.H. Ueng, Y.S. Chen, J.P. Chiu, Production of glass–ceramic from incinerator fly ash, Ceram. Int. 28 (2002) 779–783.
[29] A. Pollettini, R. Pomi, L. Trinci, A. Muntoni, S.L. Mastro, Engineering and environmental properties of thermally treated mixtures containing MSWI fly ash and low-cost additives, Chemosphere 56 (2004) 901–910.
[30] P. Kavouras, Ph. Komniou, K. Crissafis, G. Kaimakamis, S. Kokkou, K. Paraskevopoulos, Th. Karakostas, Microstructural changes of processed vitrified solid waste products, J. Eur. Ceram. Soc. 23 (2003) 1305–1311.
[31] T.W. Cheng, Combined glassification of EAF dust and incinerator fly ash, Chemosphere 50 (2003) 47–51.